

## Supporting Information

### **Li<sub>x</sub>SiON (x = 2, 4, 6); A Novel Solid Electrolyte System Derived from Agricultural Waste.**

*Xinyu Zhang, Eleni Temeche, Richard M. Laine\**

Dept. of Materials Science and Engineering, University of Michigan, Ann Arbor, MI 48109-2136, USA.

E-mail: [talsdad@umich.edu](mailto:talsdad@umich.edu)

### **Supplemental Experimental Procedures**

#### Rice hull ash (RHA) impurity removal

RHA (200 g) was milled mechanically for 48 h in a 2 L bottle with 200 g of milling media (yttria-stabilized zirconia, diameter = 3 mm) and 2 L of HCl solution (3.7 wt.% HCl). Thereafter, the acid milled RHA was recovered by suction filtration through a Buchner funnel. The recovered RHA was then washed with 500 mL deionized water.

Thereafter, the acid milled RHA and 1 L of deionized water were introduced to a 2 L glass flask equipped with a stir bar and a reflux condenser. The mixture was boiled for 24 h before separation by filtration through a Buchner funnel. The boiling and filtration processes were repeated. After the second filtration, the filtered water was confirmed neutral by pH test. The treated RHA was dried at 60 °C/vacuum/overnight and characterized by TGA-DTA (Figure **S1a**).

#### **Analytical methods**

Matrix-assisted laser desorption/ionization-time of flight (MALDI-ToF) was done on a Bruker AutoFlex Speed MALDI-TOF, both negative- and positive-ion reflectron modes were used. Trihydroxyanthracene was used as the matrix. Samples were prepared by mixing solutions of the matrix (10 mg mL<sup>-1</sup> in THF) and precursor solution (1 mg mL<sup>-1</sup> in THF), 1:1 volumetric ratio, and blotting the mixture on the target plate (MSP 96 polished steel BC, Bruker). For positive-ion mode, a AgNO<sub>3</sub> solution (1 mg mL<sup>-1</sup> in THF) is added (AgNO<sub>3</sub>:matrix = 1:5 vol.) as the ion source. The calculation of polymer precursor structures based on MALDI was done by a Python program *MALDI-Calculatation* written by Andrew Alexander, see Appendix below for details and <https://github.com/haveamission/MALDI-Calculatation> for the newest version and instructions.

Fourier-transform infrared spectroscopy (FTIR) was run on a Nicolet 6700 Series FTIR spectrometer (Thermo Fisher Scientific, Inc.). Samples (1 wt. %) were mixed with KBr powder (400 mg, Alfa Aesar); the mixtures were ground rigorously with an alumina mortar pestle, and the

dilute samples were packed in a metal sample holder to be analyzed. Prior to data acquisition in the range of 4000-400  $\text{cm}^{-1}$ , the sample chamber (rubber sealed) was purged with  $\text{N}_2$  for 10-20 min.

Thermogravimetric analysis (TGA) and differential thermal analysis (DTA) were performed on an SDT Q600 series simultaneous TGA/DTA (TA instrument, Inc.). Samples (10-20 mg) were hand-pressed in a 3-mm dual-action die and placed in alumina pans; the experiments ramped to 800 °C at 10 °C  $\text{min}^{-1}$  under constant  $\text{N}_2$  flow (60  $\text{mL min}^{-1}$ ).

Nuclear magnetic resonance spectroscopy (NMR). Vacuum dried (60 °C/1 h) precursor samples were dissolved in  $\text{CDCl}_3$  (0.1  $\text{g mL}^{-1}$ ) allowing NMR studies. All NMR spectra were recorded on a Varian vnmrs 500 MHz spectrometer.  $^7\text{Li}$  NMR spectra were collected using a spectral width of 39 kHz, a relaxation delay of 0.1 s, 32 k data points, a pulse width of 250. An aqueous solution of  $\text{LiCl}$  (9.7 M) was used as the reference ( $\delta = 0$  ppm).  $^1\text{H}$  NMR spectra were collected using a spectral width of 6 kHz, a relaxation delay of 0.5 s, 30 k data points, a pulse width of 38, and  $\text{CHCl}_3$  (7.26 ppm) as the internal reference.  $^{13}\text{C}$  NMR spectra were collected using a spectral width of 30 kHz, a relaxation delay of 0.1 s, 32 k data points, a pulse width of 250, and  $\text{CHCl}_3$  (77.16 ppm) as the internal reference.  $^{29}\text{Si}$  NMR spectra were collected using a spectral width of 20 kHz, a relaxation delay of 2.0 s, 16 k data points, a pulse width of 2.5. Tetramethylsilane (TMS,  $\delta = 0$  ppm) was used as the reference for  $^1\text{H}$ ,  $^{13}\text{C}$  and  $^{29}\text{Si}$  NMR spectra.

X-ray diffraction (XRD) was performed on dried precursor powders (60 °C/1 h/vacuum) by Rigaku MiniFlex 600 XRD and Rigaku Smartlab XRD spectrometers (Rigaku Denki., LTD., Tokyo, Japan).  $\text{Cu K}\alpha$  ( $\lambda = 1.54 \text{ \AA}$ ) radiation operates at a working voltage of 40 kV and currents of 15 and 44 mA. Scans were continuous from 10 to 80 °  $2\theta$  using a scan rate of 5 °  $\text{min}^{-1}$  in 0.01 increments. The presence of crystallographic phases was determined by using Rigaku PDXL II (version 2.8.4.0) and Expo2014 (version 1.20.03).

X-ray photoelectron spectroscopy (XPS) experiments were carried out on a Kratos Axis Ultra XPS system at room temperature bellow  $10^{-7}$  Torr using monochromatic Al source (14 kV and 8 mA). The binding energies of all the elements were calibrated relative to the gold with  $\text{Au } 4f_{7/2}$  at 84 eV. All the data were analyzed by CASAXPS software using linear type background.

Scanning electron microscopy (SEM) and energy-dispersive X-ray spectroscopy (EDX). JSM-IT300HR In Touch Scope SEM (JEOL USA, Inc.) was used to analyze the microstructures and elemental compositions of polymer precursor pellets (pelletized hydraulically at 10 ksi/20 sec with a 13 mm diameter die).

Density measurement. Masses ( $m$ ) and dimensions (thickness  $t$ , and diameter  $D$ ) of polymer precursor pellets (pelletized hydraulically at 10 ksi/20 sec with a 13 mm diameter die) heated to different temperatures were measured. Density is calculated by the equation  $\rho = 4m/(\pi D^2 t)$ .

Electrochemical impedance spectroscopy (EIS). AC impedance data were collected with a broadband dielectric spectrometer (Biologics) in a frequency range of 7 MHz to 1 Hz. “EIS spectrum analyser” software was used for extracting total resistance. Concentric Au/Pd electrodes (3 mm in diameter) were deposited using an SPI sputter coater on both surfaces of the  $\text{Li}_x\text{SiON}$  pellets using a deposition mask. An equivalent circuit consisting of  $(R_{\text{total}}Q_{\text{total}})(Q_{\text{electrode}})$  was used to measure the ionic resistivity.  $R$  and  $Q$  denote resistance and constant phase element, respectively. The total conductivity ( $\sigma_t$ ) was calculated using the equation  $\sigma_t = t/(A \times R)$ , where  $t$  is the thickness of the polymer precursor pellet (0.2-0.3 mm),  $A$  is the active area of the polymer precursor, and  $R$  is the total resistivity obtained from the Nyquist plots.

## Supplemental Data

**Table S1.** Ionic conductivities ( $\sigma$ ) and activation energies ( $E_a$ ) for  $\text{Li}_{3+x}\text{PO}_{4-x}\text{N}_x$ ,  $\text{Li}_{3+x}\text{VO}_{4-x}\text{N}_x$ ,  $\text{Li}_{2+y}\text{ZnSiO}_{4-y}\text{N}_y$  and  $\text{Li}_{2+y}\text{MgSiO}_{4-y}\text{N}_y$  solid solutions.<sup>1</sup>

Solid solution system	Composition	$\sigma$ (S cm <sup>-1</sup> ) at T °C	$E_a$ (eV)
$\text{Li}_{3+x}\text{PO}_{4-x}\text{N}_x$	$\text{Li}_3\text{PO}_4$	$1.0 \times 10^{-18}$ (25)	1.18
	$\text{Li}_{3.2}\text{PO}_{3.8}\text{N}_{0.2}$	$9.6 \times 10^{-15}$ (25)	0.92
	$\text{Li}_{3.4}\text{PO}_{3.6}\text{N}_{0.4}$	<b><math>2.5 \times 10^{-14}</math> (25)</b>	<b>0.91</b>
	$\text{Li}_{3.6}\text{PO}_{3.4}\text{N}_{0.6}$	$2.0 \times 10^{-16}$ (25)	1.20
	$\text{Li}_{3.8}\text{PO}_{3.2}\text{N}_{0.8}$	$1.6 \times 10^{-16}$ (25)	1.18
$\text{Li}_{3+x}\text{VO}_{4-x}\text{N}_x$	$\text{Li}_3\text{VO}_4$	$2.0 \times 10^{-7}$ (360)	1.29
	$\text{Li}_{3.2}\text{VO}_{3.8}\text{N}_{0.2}$	<b><math>4.0 \times 10^{-4}</math> (330)</b>	<b>1.00</b>
	$\text{Li}_{3.4}\text{VO}_{3.6}\text{N}_{0.4}$	$1.2 \times 10^{-5}$ (330)	1.01
	$\text{Li}_{3.6}\text{VO}_{3.4}\text{N}_{0.6}$	$3.0 \times 10^{-5}$ (330)	1.02
$\text{Li}_{2+y}\text{ZnSiO}_{4-y}\text{N}_y$	$\text{Li}_2\text{ZnSiO}_4$	$8.0 \times 10^{-8}$ (390)	1.14
	$\text{Li}_{2.2}\text{ZnSiO}_{3.8}\text{N}_{0.2}$	$8.0 \times 10^{-8}$ (115)	0.99
	$\text{Li}_{2.4}\text{ZnSiO}_{3.6}\text{N}_{0.4}$	<b><math>4.0 \times 10^{-6}</math> (125)</b>	<b>0.44</b>
	$\text{Li}_{2.6}\text{ZnSiO}_{3.4}\text{N}_{0.6}$	<b><math>2.0 \times 10^{-6}</math> (70)</b>	<b>0.55</b>
$\text{Li}_{2+y}\text{MgSiO}_{4-y}\text{N}_y$	$\text{Li}_2\text{MgSiO}_4$	$4.0 \times 10^{-8}$ (420)	1.39
	$\text{Li}_{2.2}\text{MgSiO}_{3.8}\text{N}_{0.2}$	$4.0 \times 10^{-7}$ (115)	0.80
	$\text{Li}_{2.4}\text{MgSiO}_{3.6}\text{N}_{0.4}$	$1.0 \times 10^{-6}$ (130)	0.87
	$\text{Li}_{2.6}\text{MgSiO}_{3.4}\text{N}_{0.6}$	<b><math>7.0 \times 10^{-6}</math> (130)</b>	<b>0.83</b>
	$\text{Li}_{2.8}\text{MgSiO}_{3.2}\text{N}_{0.8}$	<b><math>5.0 \times 10^{-7}</math> (110)</b>	<b>0.79</b>

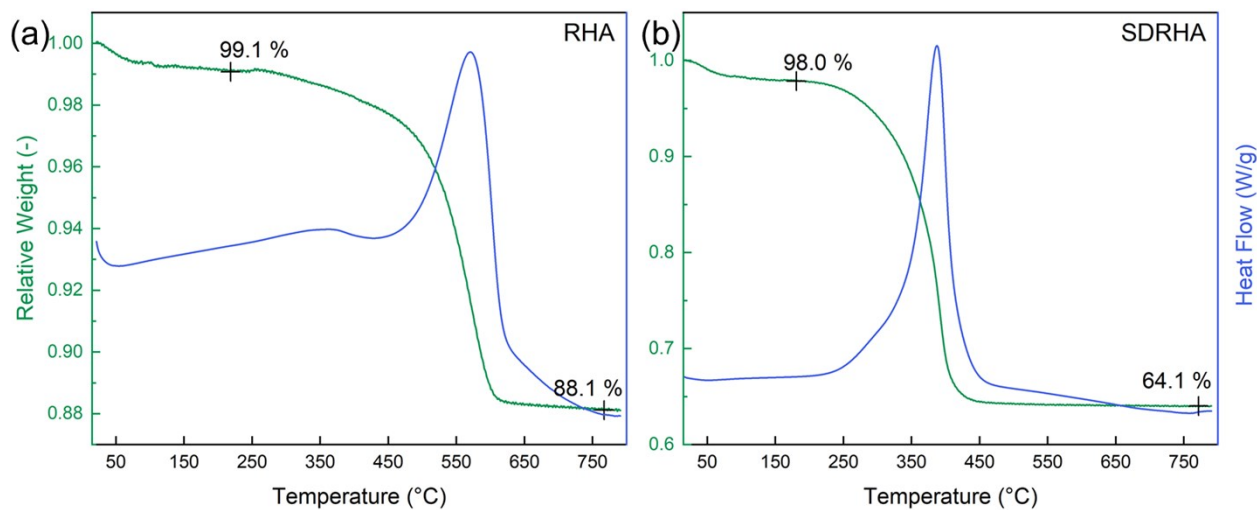


**Figure S1.** TGA-DTAs (800 °C/10 °C min<sup>-1</sup>/air) of **a.** acid purified RHA and **b.** silica depleted RHA (SDRHA).

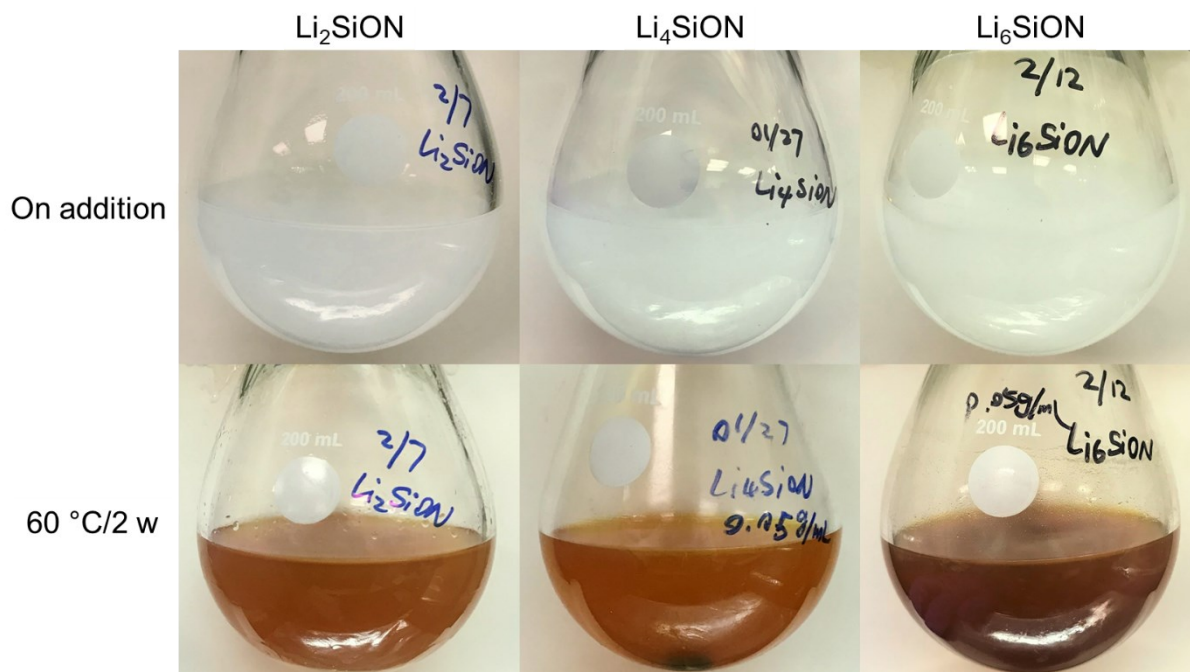


**Figure S2.** Typical syntheses of  $\text{Li}_x\text{SiON}$  precursors.

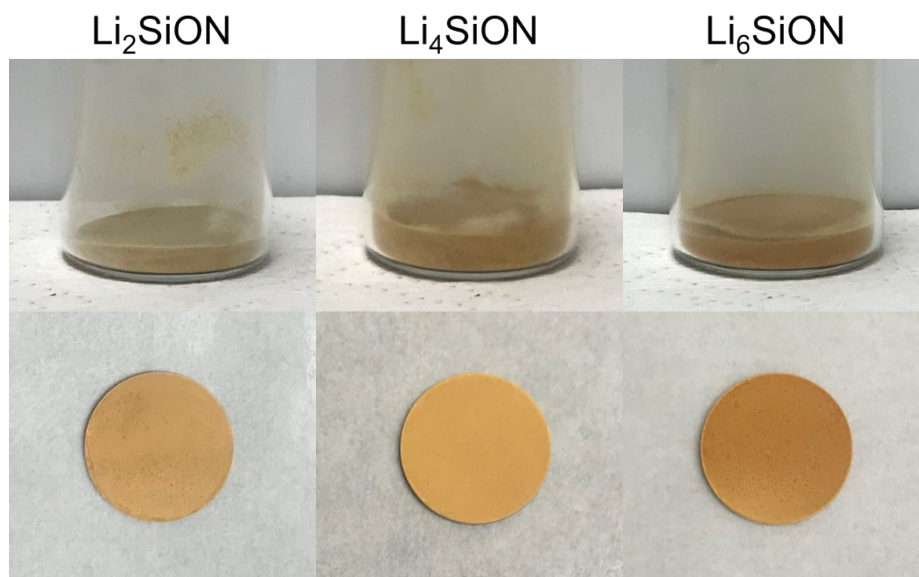


**Figure S3.** Optical images of representative dried  $\text{Li}_x\text{SiON}$  precursor powders (top) and hydraulically pressed pellets (bottom, 10 ksi/20 sec with a 13 mm diameter die).

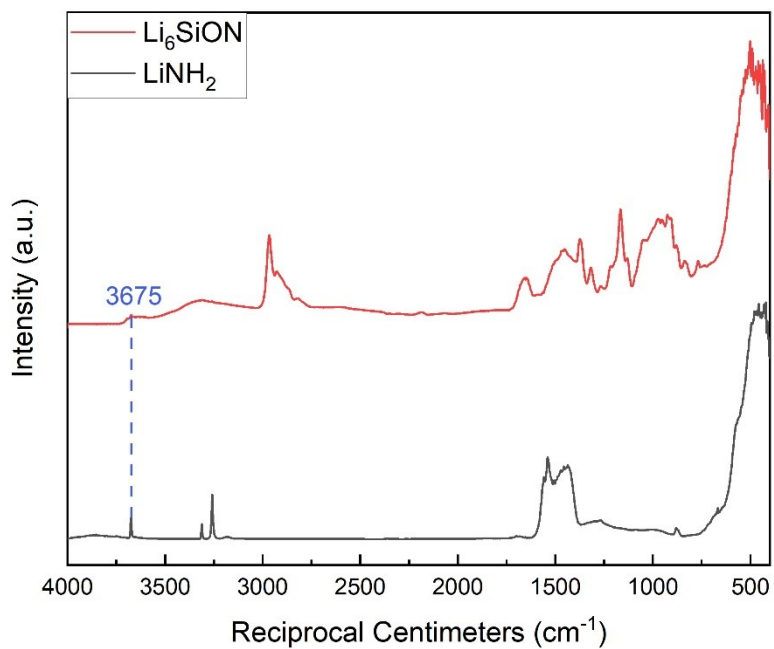


**Figure S4.** FTIRs of  $\text{Li}_6\text{SiON}$  (dried at 60 °C/1 h/vacuum) and  $\text{LiNH}_2$ .

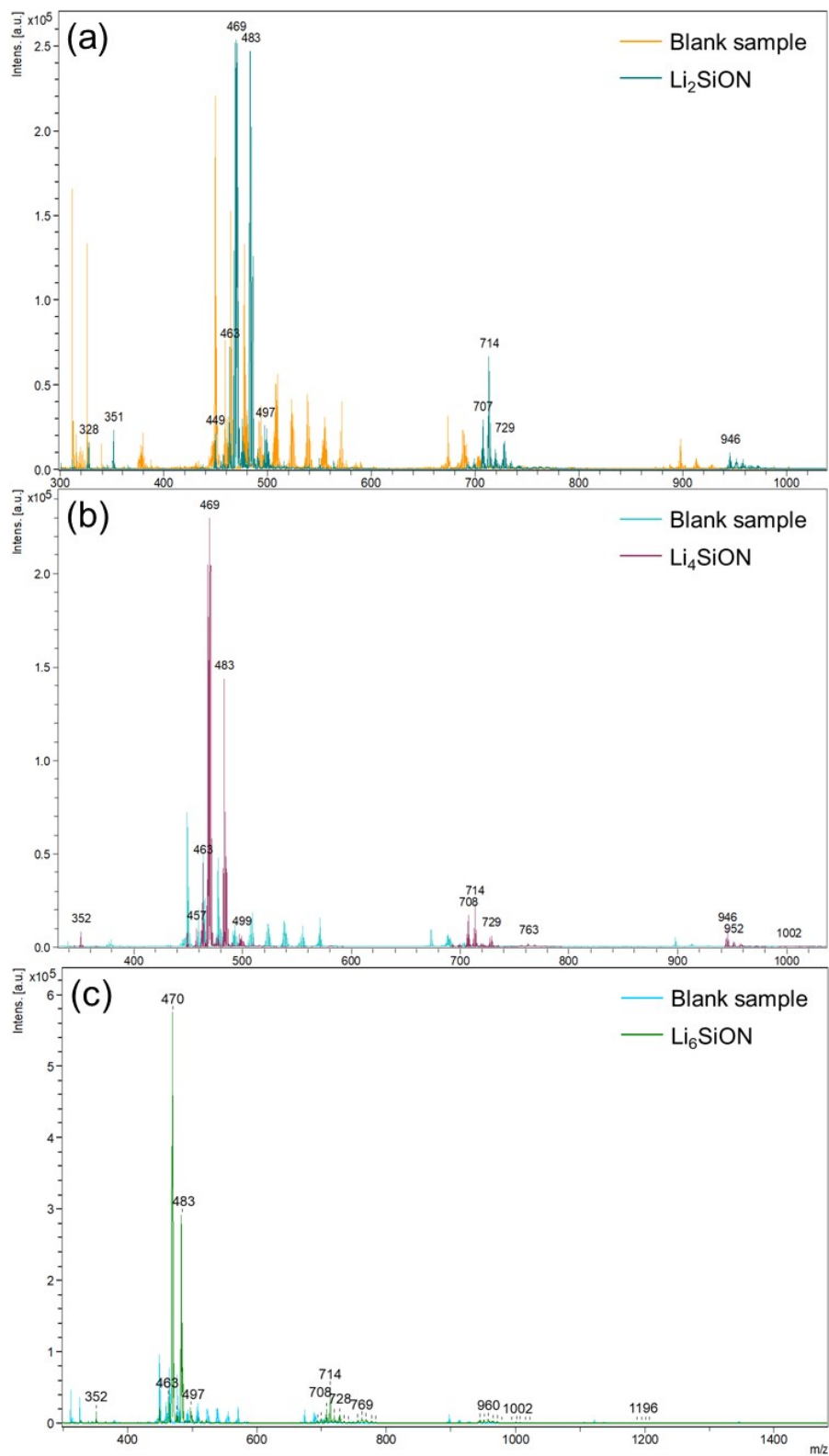


**Figure S5.** Negative-ion mode MALDIs of blank vs  $\text{Li}_x\text{SiON}$  precursors, **a.**  $\text{Li}_2\text{SiON}$ , **b.**  $\text{Li}_4\text{SiON}$  and **c.**  $\text{Li}_6\text{SiON}$ .

**Table S2.** Possible compositions of  $\text{Li}_x\text{SiON}$  precursors based on MALDI.<sup>†</sup>

Precursor	Positive-ion mode			Negative-ion mode		
	Group	m/z	Calculation	Group	m/z	Calculation
$\text{Li}_2\text{SiON}$	I	342	$\text{S} + 2\text{A} + 7\text{L} = 341.0$	I	328	$\text{S} + 2\text{A} + 5\text{L} = 327.2$
		472	$\text{S} + 8\text{A} + 12\text{L} = 471.8$		351	$\text{S} + 3\text{A} + 6\text{L} = 350.1$
	II	484	$\text{S} + 7\text{A} + 16\text{L} = 483.6$	II	449	$\text{S} + 10\text{A} + 4\text{L} = 448.4$
		505	$\text{S} + 11\text{A} + 10\text{L} = 506.1$		463	$\text{S} + 7\text{A} + 13\text{L} = 462.8$
		539	$\text{S} + 10\text{A} + 17\text{L} = 538.6$		469	$\text{S} + 10\text{A} + 7\text{L} = 469.2$
		555	$\text{S} + 11\text{A} + 17\text{L} = 554.6$		483	$\text{S} + 10\text{A} + 9\text{L} = 483.1$
		722	$2\text{S} + 10\text{A} + 6\text{L} = 722.7$		497	$\text{S} + 10\text{A} + 11\text{L} = 497.0$
	III	728	$2\text{S} + 9\text{A} + 9\text{L} = 727.5$	III	707	$2\text{S} + 9\text{A} + 6\text{L} = 706.6$
		767	$2\text{S} + 11\text{A} + 10\text{L} = 766.5$		714	$2\text{S} + 9\text{A} + 7\text{L} = 713.6$
		773	$2\text{S} + 11\text{A} + 11\text{L} = 773.4$		729	$2\text{S} + 10\text{A} + 7\text{L} = 729.6$
	IV	960	$3\text{S} + 6\text{A} + 12\text{L} = 960.6$	IV	946	$3\text{S} + 9\text{A} + 3\text{L} = 946.2$
		966	$3\text{S} + 5\text{A} + 15\text{L} = 965.4$			
		1012	$3\text{S} + 7\text{A} + 17\text{L} = 1011.4$			
$\text{Li}_4\text{SiON}$	I	314	$\text{S} + 2\text{A} + 3\text{L} = 313.3$	I	352	$\text{S} + 4\text{A} + 4\text{L} = 352.2$
		352	$\text{S} + 4\text{A} + 4\text{L} = 352.2$		457	$\text{S} + 8\text{A} + 10\text{L} = 458.0$
	II	472	$\text{S} + 8\text{A} + 12\text{L} = 471.8$	II	463	$\text{S} + 7\text{A} + 13\text{L} = 462.8$
		478	$\text{S} + 8\text{A} + 13\text{L} = 478.8$		469	$\text{S} + 10\text{A} + 7\text{L} = 469.2$
		484	$\text{S} + 7\text{A} + 16\text{L} = 483.6$		483	$\text{S} + 10\text{A} + 9\text{L} = 483.1$
		722	$2\text{S} + 10\text{A} + 6\text{L} = 722.7$		499	$\text{S} + 11\text{A} + 9\text{L} = 499.1$
	III	728	$2\text{S} + 9\text{A} + 9\text{L} = 727.5$	III	708	$2\text{S} + 6\text{A} + 13\text{L} = 707.2$
		738	$2\text{S} + 11\text{A} + 6\text{L} = 738.7$		714	$2\text{S} + 9\text{A} + 7\text{L} = 713.6$
		767	$2\text{S} + 11\text{A} + 10\text{L} = 766.5$		729	$2\text{S} + 10\text{A} + 7\text{L} = 729.6$
		960	$3\text{S} + 6\text{A} + 12\text{L} = 960.6$		763	$2\text{S} + 9\text{A} + 14\text{L} = 762.2$
	IV	966	$3\text{S} + 5\text{A} + 15\text{L} = 965.4$	IV	946	$3\text{S} + 9\text{A} + 3\text{L} = 946.2$
		1006	$3\text{S} + 8\text{A} + 14\text{L} = 1006.6$		952	$3\text{S} + 5\text{A} + 13\text{L} = 951.6$
		1204	$4\text{S} + 8\text{A} + 5\text{L} = 1204.5$		1002	$3\text{S} + 9\text{A} + 11\text{L} = 1001.8$
	V	1251	$4\text{S} + 7\text{A} + 14\text{L} = 1250.9$			
$\text{Li}_6\text{SiON}$	I	472	$\text{S} + 8\text{A} + 12\text{L} = 471.8$	I	352	$\text{S} + 4\text{A} + 4\text{L} = 352.2$
		478	$\text{S} + 8\text{A} + 13\text{L} = 478.8$		463	$\text{S} + 7\text{A} + 13\text{L} = 462.8$
		484	$\text{S} + 7\text{A} + 16\text{L} = 483.6$		470	$\text{S} + 10\text{A} + 7\text{L} = 469.2$
	II	722	$2\text{S} + 10\text{A} + 6\text{L} = 722.7$	II	483	$\text{S} + 10\text{A} + 9\text{L} = 483.1$
		728	$2\text{S} + 9\text{A} + 9\text{L} = 727.5$		497	$\text{S} + 10\text{A} + 11\text{L} = 497.0$
		767	$2\text{S} + 11\text{A} + 10\text{L} = 766.5$		708	$2\text{S} + 6\text{A} + 13\text{L} = 707.2$
	III	960	$3\text{S} + 6\text{A} + 12\text{L} = 960.6$	III	714	$2\text{S} + 9\text{A} + 7\text{L} = 713.6$
		965	$3\text{S} + 8\text{A} + 8\text{L} = 964.9$		728	$2\text{S} + 9\text{A} + 9\text{L} = 727.5$
		1006	$3\text{S} + 8\text{A} + 14\text{L} = 1006.6$		769	$2\text{S} + 9\text{A} + 15\text{L} = 769.1$
		1198	$4\text{S} + 5\text{A} + 11\text{L} = 1198.1$		960	$3\text{S} + 6\text{A} + 12\text{L} = 960.6$
	IV	1244	$4\text{S} + 7\text{A} + 13\text{L} = 1244.0$	IV	1002	$3\text{S} + 9\text{A} + 11\text{L} = 1001.8$
	V	1436	$5\text{S} + 4\text{A} + 10\text{L} = 1435.5$	V	1196	$4\text{S} + 4\text{A} + 13\text{L} = 1195.9$

<sup>†</sup> S = spiroxiloxane, A =  $-\text{NH}_2$ , L =  $\text{Li}^+$ . All possible compositions are calculated by Python program *MALDI-Calculat*ion (see Appendix below): <https://github.com/haveamission/MALDI-Calculat>ion.

Li<sub>6</sub>SiON

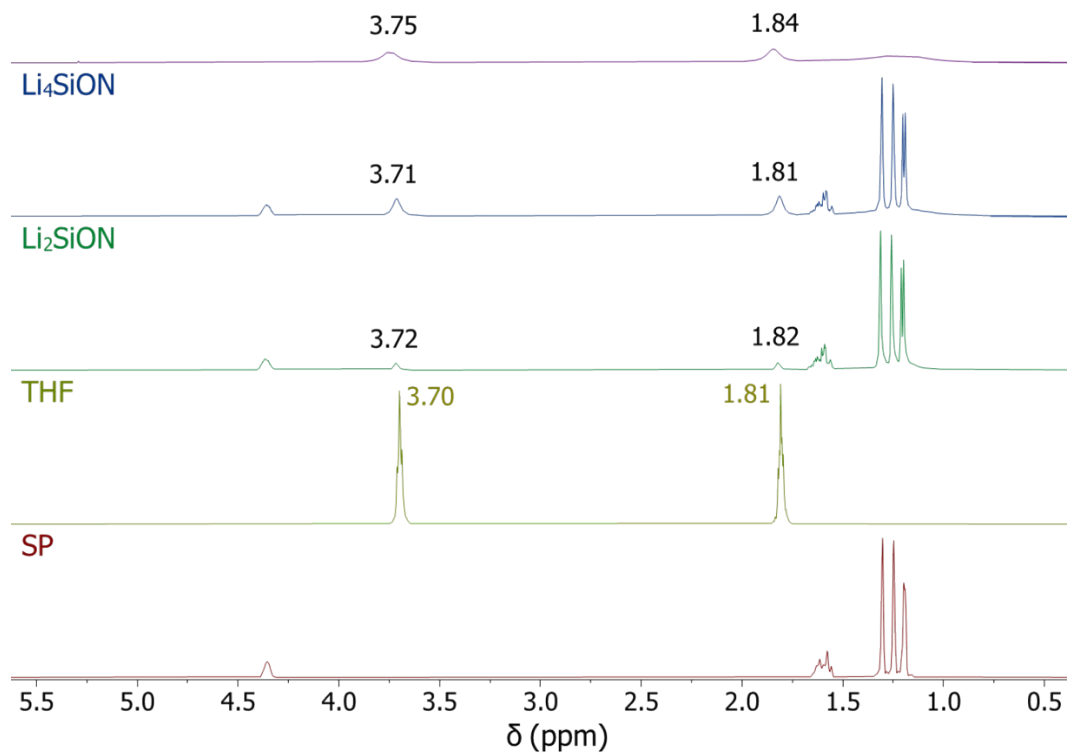


**Figure S6.** <sup>1</sup>H NMRs of Li<sub>x</sub>SiON precursors (RT/1 h/vacuum), THF and SP.

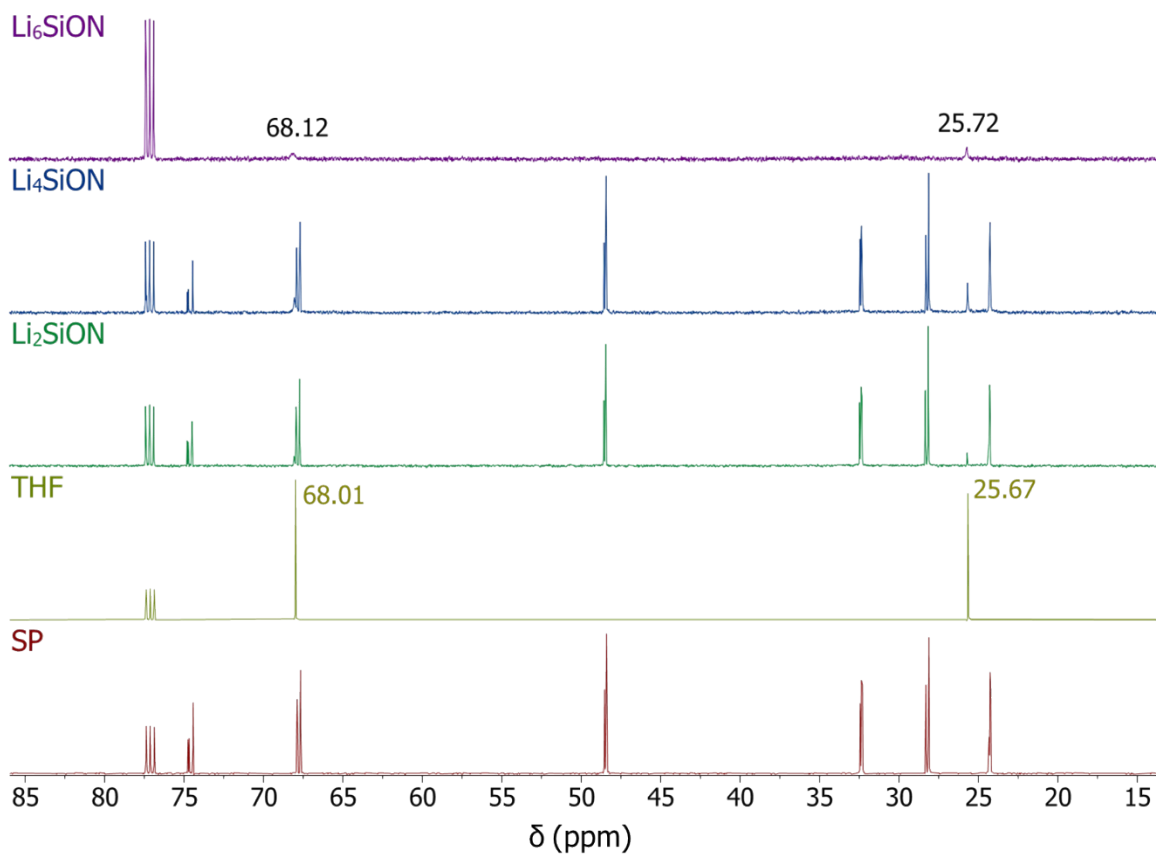


**Figure S7.**  $^{13}\text{C}$  NMRs of  $\text{Li}_x\text{SiON}$  precursors (RT/1 h/vacuum), THF and SP.

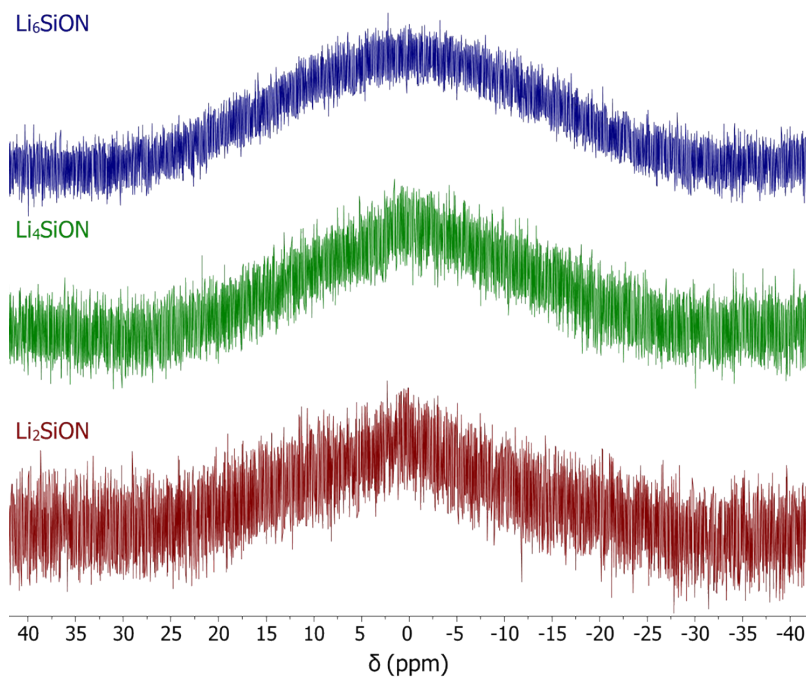


**Figure S8.**  $^7\text{Li}$  NMRs of  $\text{Li}_x\text{SiON}$  precursors (60  $^\circ\text{C}$ /24 h/vacuum).

(a)  $\text{Li}_6\text{SiON}$

(b)  $\text{Li}_6\text{SiON}$

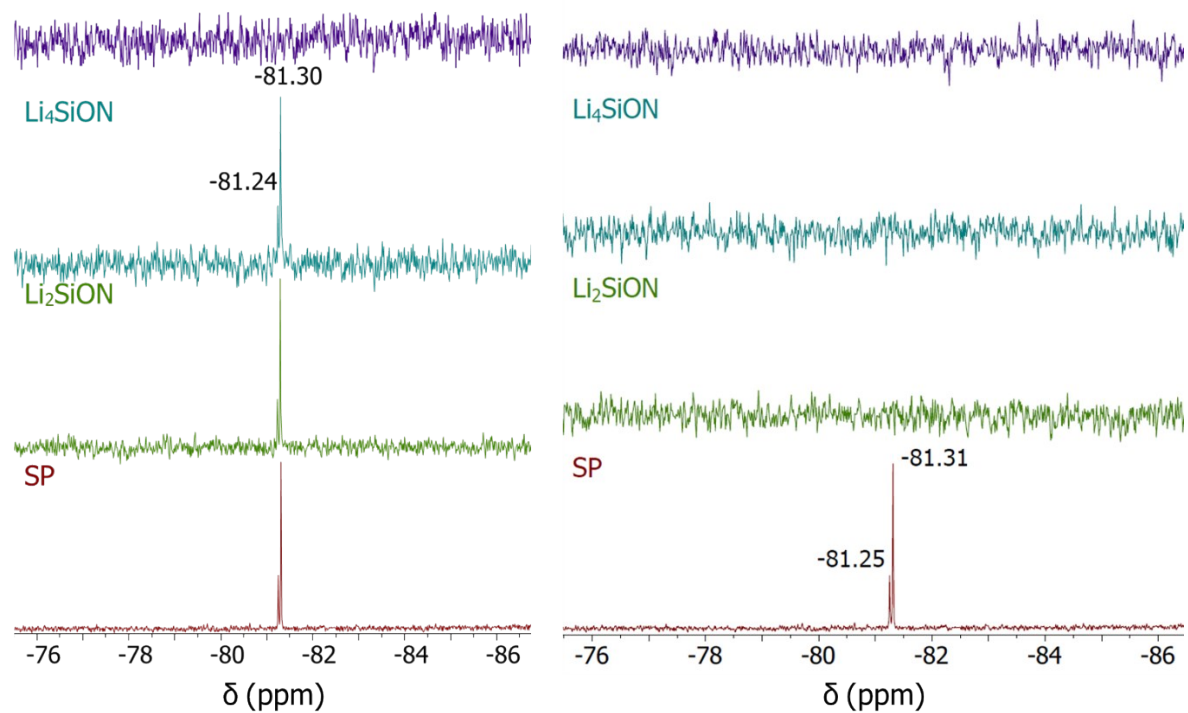


**Figure S9.**  $^{29}\text{Si}$  NMRs of  $\text{Li}_x\text{SiON}$  precursors dried at **a.** RT/1 h/vacuum and **b.** 60 °C/24 h/vacuum.

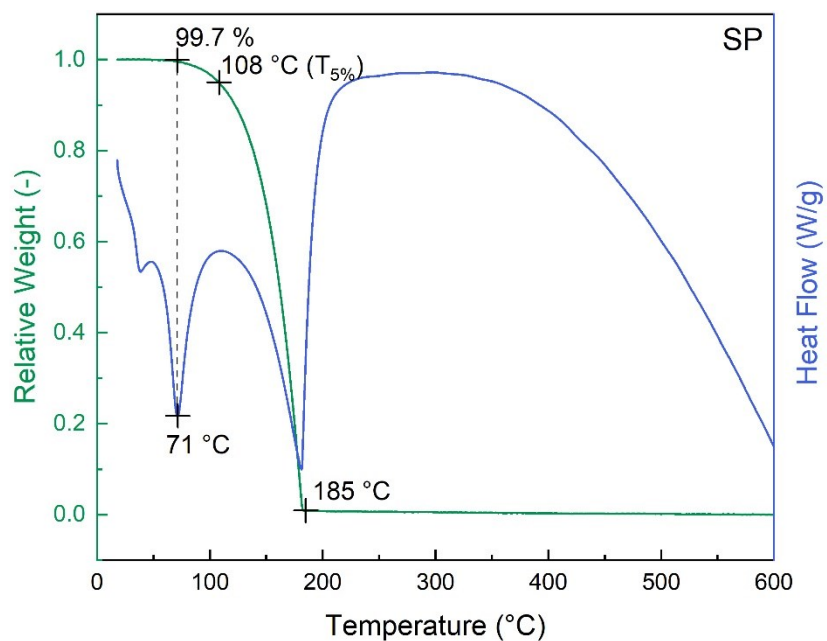


**Figure S10.** TGA-DTA (600 °C/10 °C  $\text{min}^{-1}/\text{N}_2$ ) of SP (60 °C/12 h/vacuum).

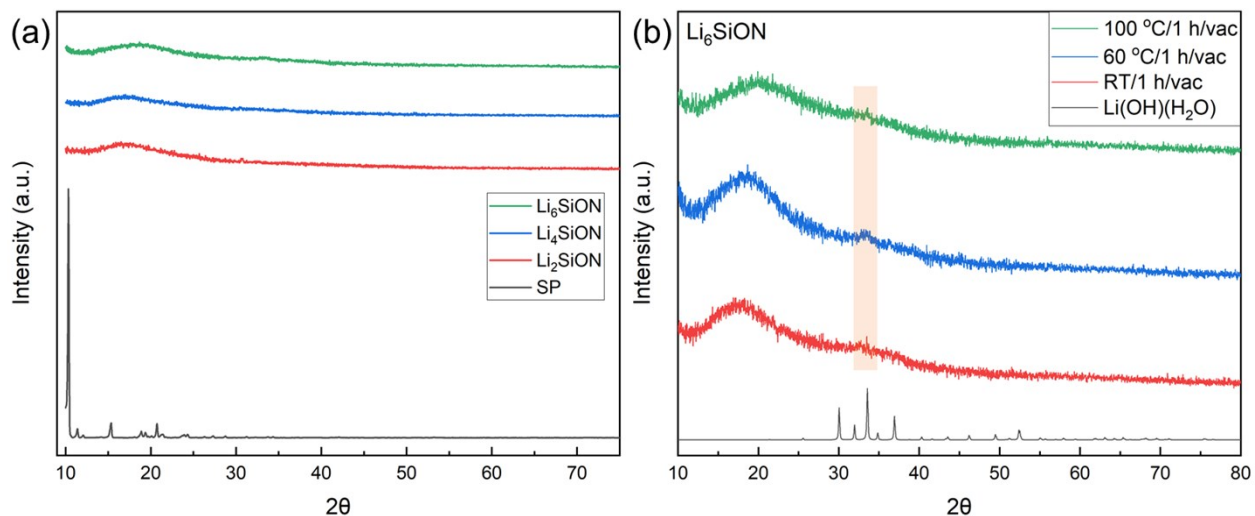


**Figure S11.** XRDs of **a.**  $\text{Li}_x\text{SiON}$  precursors (60 °C/1 h/vacuum) and SP (60 °C/12 h/vacuum), **b.**  $\text{Li}_6\text{SiON}$  dried at RT, 60° and 100 °C/1 h/vacuum.

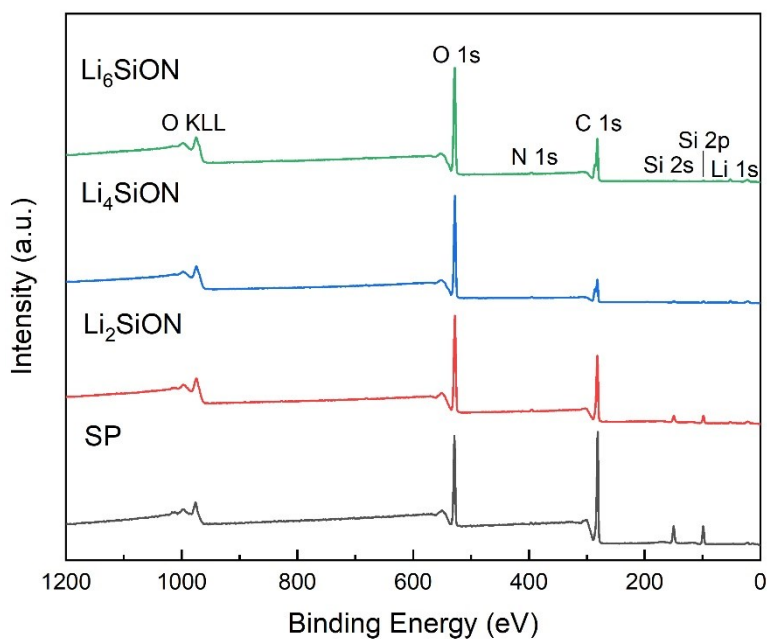


**Figure S12.** Wide-scan survey XPS spectra of  $\text{Li}_x\text{SiON}$  precursors dried at RT/1 h/vacuum compared to SP (60 °C/12 h/vacuum).

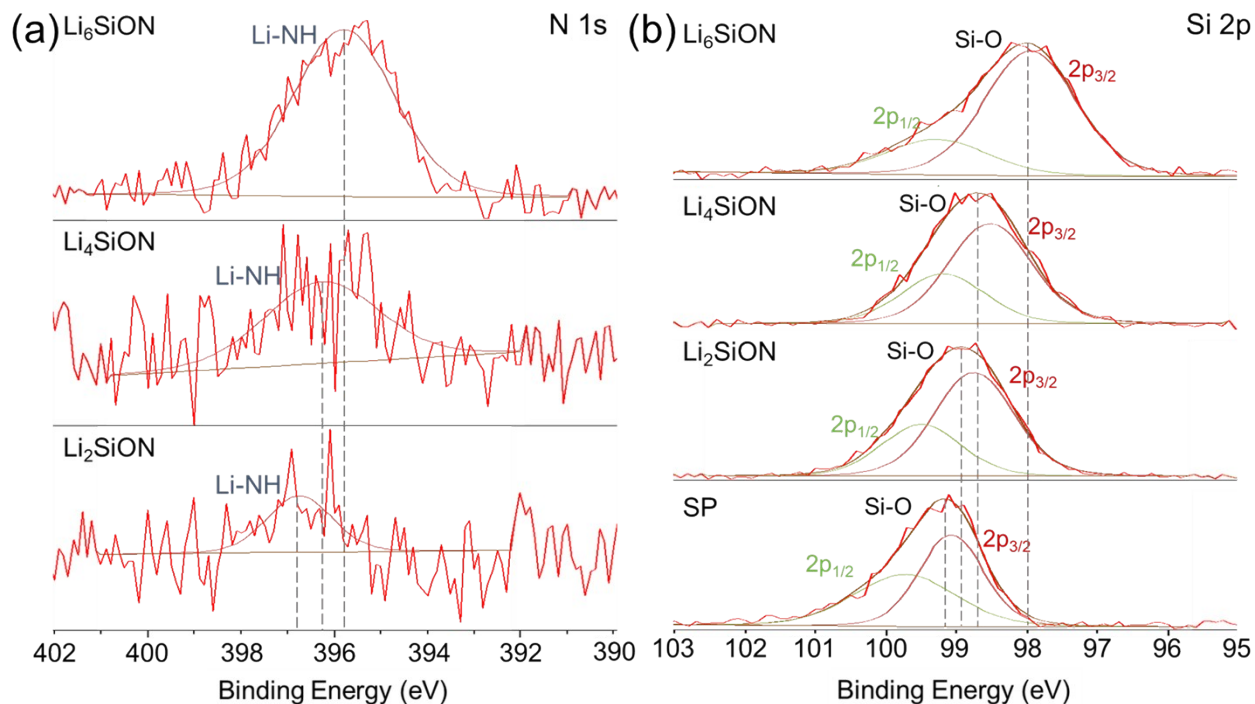


**Figure S13.** N 1s core-level XPS spectra of  $\text{Li}_x\text{SiON}$  precursors (60 °C/1 h/vacuum). **b.** Si 2p XPS core-level spectra of  $\text{Li}_x\text{SiON}$  precursors (60 °C/1 h/vacuum) compared to SP (60 °C/12 h/vacuum).

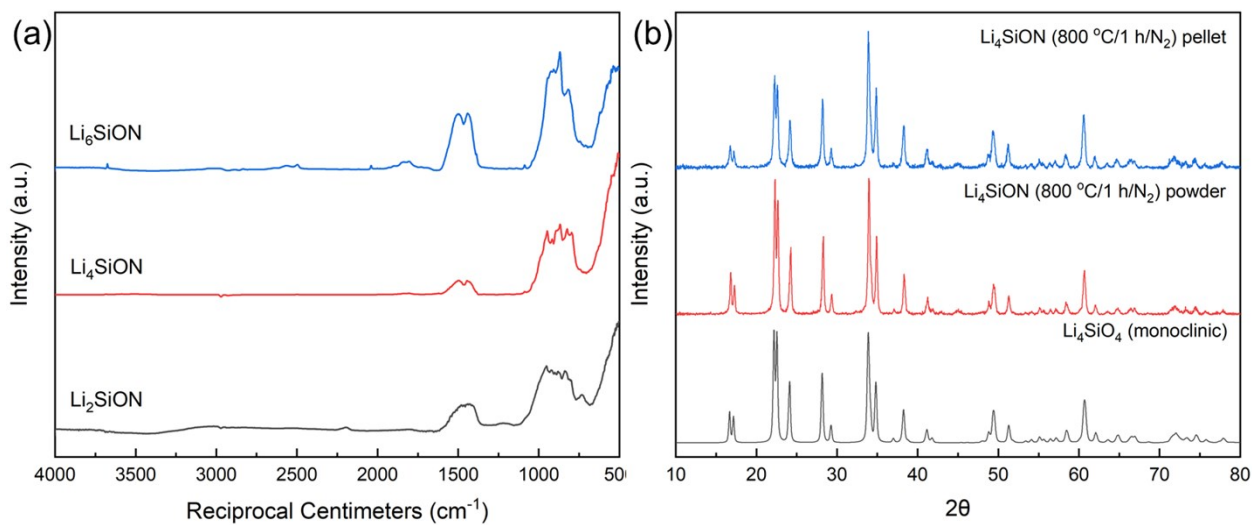


**Figure S14.** **a.** FTIRs of  $\text{Li}_x\text{SiON}$  pellets heated to 800 °C/1 h/ $\text{N}_2$ . **b.** XRDs of  $\text{Li}_4\text{SiON}$  (800 °C/1 h/ $\text{N}_2$ ) pellet and powder compared to  $\text{Li}_4\text{SiO}_4$  (monoclinic).

**Table S3.** Densities ( $\text{g}/\text{cm}^3$ ) of  $\text{Li}_x\text{SiON}$  precursors treated under different conditions.

	$\text{Li}_2\text{SiON}$	$\text{Li}_4\text{SiON}$	$\text{Li}_6\text{SiON}$
60 °C/1 h/vacuum	$0.96 \pm 0.06$	$1.04 \pm 0.04$	$1.11 \pm 0.06$
100 °C/2 h/ $\text{N}_2$	$1.17 \pm 0.03$	$1.35 \pm 0.06$	$1.09 \pm 0.07$
200 °C/2 h/ $\text{N}_2$	$1.23 \pm 0.03$	$1.39 \pm 0.05$	$1.31 \pm 0.04$
300 °C/2 h/ $\text{N}_2$	$1.23 \pm 0.03$	$1.46 \pm 0.03$	$1.37 \pm 0.05$
400 °C/2 h/ $\text{N}_2$	$1.21 \pm 0.04$	$1.29 \pm 0.03$	$1.41 \pm 0.04$

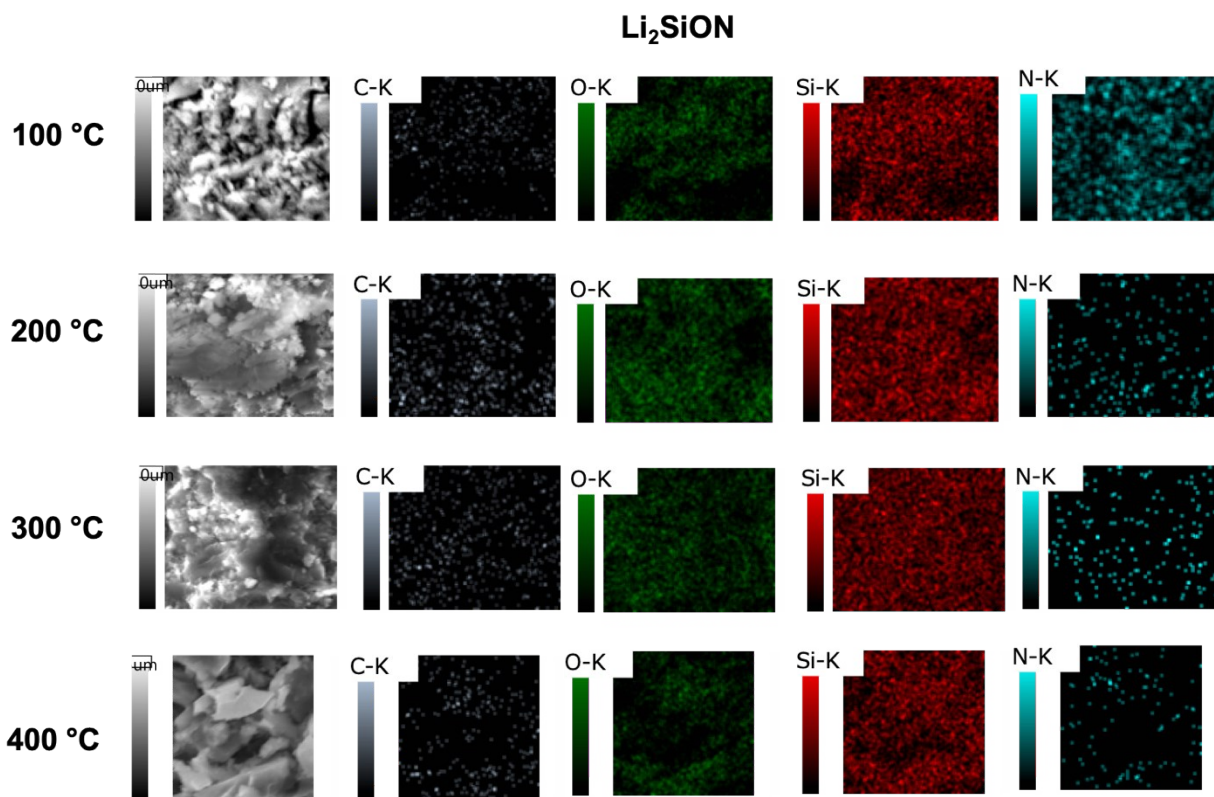


**Figure S15.** EDX map of  $\text{Li}_2\text{SiON}$  pellets heated to 100°-400 °C/2 h/  $\text{N}_2$ .

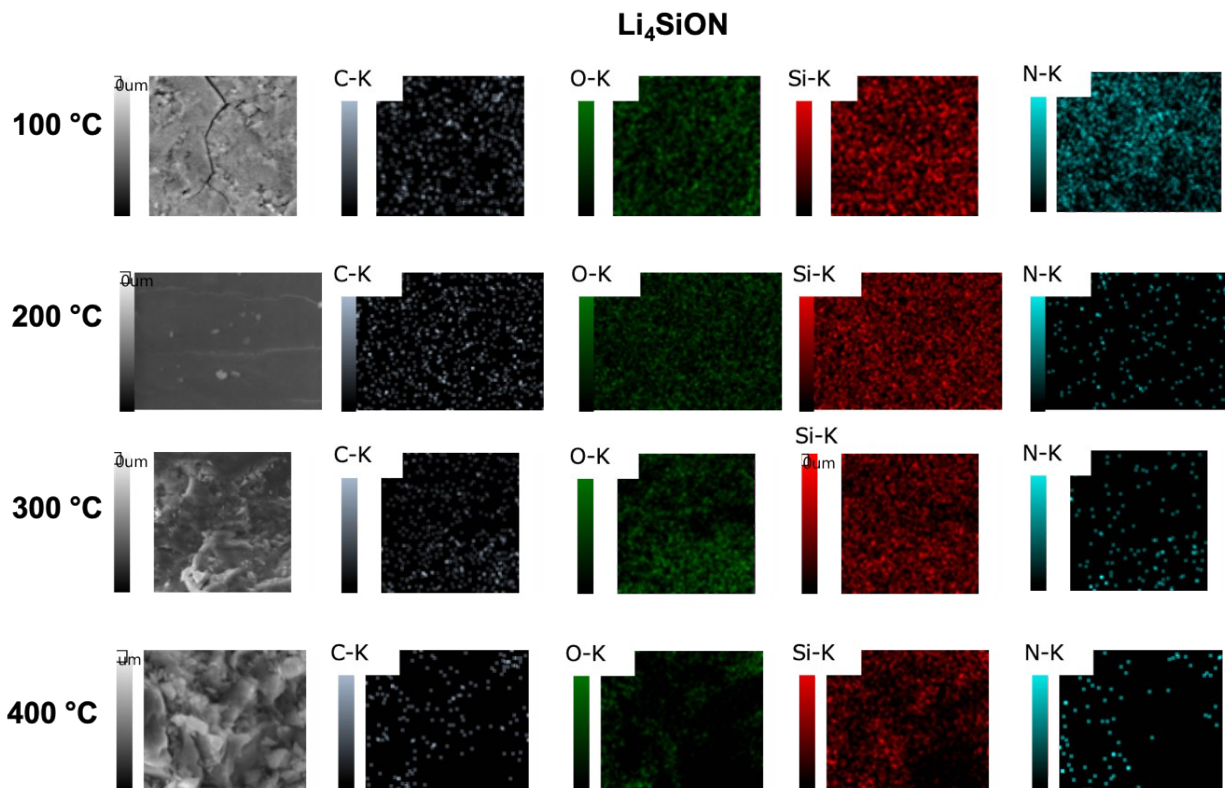


**Figure S16.** EDX map of Li<sub>4</sub>SiON pellets heated to 100°-400 °C/2 h/ N<sub>2</sub>.

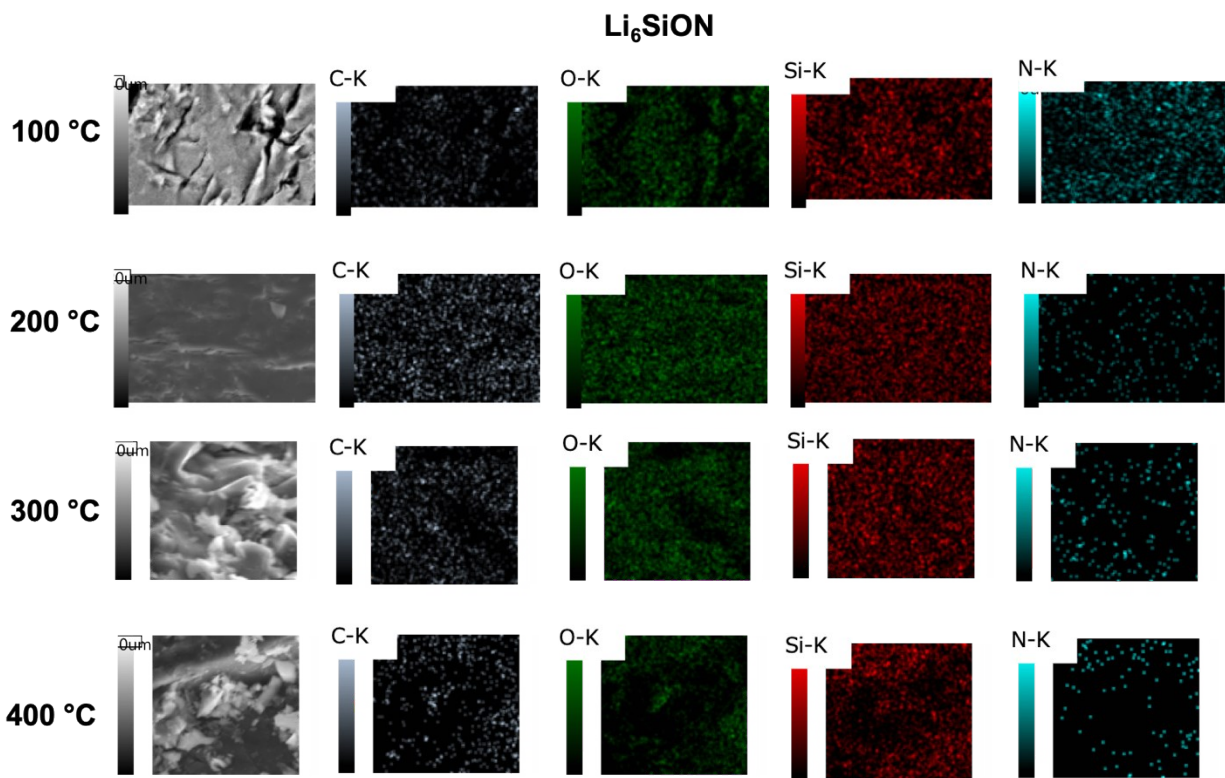


**Figure S17.** EDX map of Li<sub>6</sub>SiON pellets heated to 100°-400 °C/2 h/ N<sub>2</sub>.

**Table S4.** Average atomic percentage (At. %) of Li<sub>x</sub>SiON pellets based on EDX analyses.

	Precursor pellet	Temp. (°C/2 h)	At. %			
			C	N	O	Si
Li <sub>2</sub> SiON		100	23.2	1.8	65.2	9.8
		200	22.3	1.2	67.5	9.0
		300	21.7	1.0	67.0	10.3
		400	19.7	0.5	67.4	12.4
Li <sub>4</sub> SiON		100	27.5	1.7	64.2	6.6
		200	27.2	1.0	62.7	8.9
		300	23.6	0.5	67.5	8.4
		400	21.6	0.2	68.0	10.2
Li <sub>6</sub> SiON		100	31.6	1.1	61.6	5.7
		200	31.4	1.3	62.0	5.3
		300	30.1	0.7	64.8	4.4
		400	28.5	0.2	65.0	6.3

## Appendix

The below Python program was developed by Andrew Alexander as a tool to calculate polymer precursor structures based on MALDI-ToF study. Two files are included, one is the configuration and data set (JSON format) which needs manual inputs according to the polymer structures, the other one is the program file.

An example structural calculation of a  $\text{Li}_x\text{SiON}$  peak from MALDI-ToF is given below. Please note that this program is under constant improvement; the newest version and instructions can be found at: <https://github.com/haveamission/MALDI-Calculation>.

The program is licensed under Creative Commons Non-Commercial ShareAlike 4.0 International; third party contributions are welcomed.

### File 1, configuration and data set:

```
{
    "monomer_weight": {"S": 260.41, "A": 16.02, "L": 6.94},
    "polymer_weight": [722],
    "range_bottom": 5,
    "range_top": 30,
    "error_number":1
}
```

### File 2, main program:

```
import itertools
import json

class MolecularWeight:

    def __init__(self):
        filename = input("Enter filename: ")
        if filename:
            datastore = self.load_file(filename)
        else:
            datastore = self.load_file("default_dataset.json")
        self.monomer_weight = datastore["monomer_weight"]
```

```

self.monomer_weight_keys = self.monomer_weight.keys()
self.polymer_weight = datastore["polymer_weight"]
self.range_bottom = datastore["range_bottom"]
self.range_top = datastore["range_top"]
self.error_number = datastore["error_number"]
self.main()

def load_file(self, filename):
    with open(filename, 'r') as f:
        datastore = json.load(f)
    return datastore

def check_list(self, number, final_alpha):
    result = {}
    for monomer_weight_num in self.polymer_weight:
        if abs(monomer_weight_num - number) < self.error_number:
            result[number] = final_alpha
            return result
        else:
            pass

def use_iter(self, range_num):
    product_list =
list(itertools.combinations_with_replacement(self.monomer_weight_keys, range_num))
    return product_list

def combinations_generator(self):
    steps = []
    for range_num in range(self.range_bottom, self.range_top):
        step = self.use_iter(range_num)
        steps.extend(step)
    return steps

def result_calculator(self, combination):
    final_value = 0
    final_alpha = ""
    for item in combination:
        value = self.monomer_weight[item]

```

```
        final_value += value
        final_alpha += item
    result = self.check_list(final_value, final_alpha)
    return result

def main(self):
    combinations = self.combinations_generator()
    for combination in combinations:
        result = self.result_calculator(combination)
        if result:
            print(result)
```

MolecularWeight()

## Reference

1 R. Jarkaneh, Novel Oxynitride Lithium Ion Conductors, 2015.